Optimizing 7T Spine Array Design through Offsetting of Transmit and Receive Elements and Quadrature Excitation

Q. Duan[1], D. K. Sodickson[1], R. Lattanzi[1], B. Zhang[1], and G. C. Wiggins[1]
[1]Center for Biomedical Imaging, Department of Radiology, NYU School of Medicine, New York, NY, United States

Introduction

MRI spine imaging at 3T has been found to offer improvement over 1.5T in terms of SNR and tissue delineation, but with new challenges related to B_1 and B_0 inhomogeneity [1]. At 7T there is an additional problem of a lack of commercially available RF coils and the opposite twisting of B_1^+ and B_1^- [2] complicates coil design. Recently, Kraff *et al* demonstrated an 8 channel transceive array [3] with 2 rows of 4 coils extending along the spine, with 180° driving phase between two columns. In this work, we used full wave electromagnetic simulation and prototype coils to evaluate a number of different multi-element designs. We aimed for improved excitation efficiency and SNR within the spinal region of interest and reduced SAR. In the coil optimization, we evaluated the strategies of quadrature excitation and the offsetting of transmit (Tx) and receive (Rx) elements [4]. The B_1^+, SNR and SAR performance of the proposed designs are illustrated in phantom scans.

Methods

B_1^+ and B_1^- fields were generated using a full-wave simulation based on dyadic Green's functions [5] with a 40cm diameter cylindrical phantom with uniform dielectric properties corresponding to muscle tissue (σ=0.79 S/m ε_r=59) [6]. Six different square elements were simulated, with side lengths of 4, 6, 8, 10, 12, and 14 cm. In order to quantitatively optimize the design parameters, a ROI of 9cm depth and 8cm diameter corresponding to the spinal region was chosen as the optimization target area based on human anatomy. We evaluated different designs for individual "building blocks", which can be conveniently arranged next to each other along Z to increase coil coverage along the Z direction. Based on the simulation results, experimental validation was performed by constructing various array designs with 10cm elements made from FR4 circuit board with a 6mm conductor width as shown in Table 1. Each coil was tuned to 297.2MHz with 8 capacitors. A body mimicking phantom with the same dielectric properties as the simulated tissue was built. Standard detune circuits were used for Rx only coils providing least 30dB detune. Diodes were incorporated in series with the Tx only coils to provide at least 18dB detune. For each surface coil a T/R switch preamp device was used (Stark Contrast, Erlangen Germany), which also provided at least 17dB preamp decoupling during receive. MR experiments were performed on Siemens Magnetom 7T system. GRE sequences with 1250ms TR and various transmit voltages were used for B_1 mapping and SNR scans for different arrays were carefully calibrated with an 80° flip angle at 5cm depth.

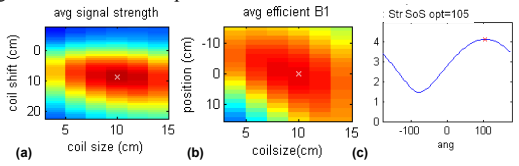

Fig. 1: Quantitative coil optimization: (a) Tx/Rx offset optimization based on signal strength; (b) Tx pair optimization based on B1 efficiency; (c) driving phase optimization based on signal strength

No	Array design
1	1 T/R coil
2	2coils: 1Tx with and 1 offseted Rx
3	2coils: 2 T/R coils with 180 driving (Kraff's system)
4	2coils: 2 T/R coils with 90 driving
5	3coils: 1Tx coil +1 T/R coil + 1Rx (Our prototype)

Table 1: Testing arrays

Results

Coil optimization: Two different optimization strategies were considered. Adopting the strategy of offsetting separate Tx and Rx elements to optimize B_1^+ and B_1^- in the ROI [4] the first step was to optimize the coil size and the corresponding offset between the Tx and Rx elements. The average signal strength [7] within the ROI was chosen as the metric. As shown in Fig.1a, the optimal coil size is 10cm and the optimal offset between the centers of two coils is 8.8cm. This happens to correspond to the case for two coils overlapped to minimize inductive coupling. The second strategy was to consider the case of two transmit-receive coils placed side by side. For each element size we varied the azimuthal position of the loop pair and then stepped through driving phases for the two loops until the maximum B1+ efficiency [8] was obtained in the ROI. Fig.1b shows the results where each data point has already been optimized for driving phase (which will not necessarily be the same for each case). The optimum is reached for a pair of 10cm elements with an offset of zero, which in our coordinate definition corresponds to the right-hand coil being centered under the ROI. The optimum driving phase for this configuration was 105° (Fig.1c), though in our practical implementation of the coil we used 90° (99% of the maximum B_1^+ efficiency). After the optimization, a basic building block can be settled as shown in the 5th row of Fig.2: three geometrically decoupled 10cm coils with the left one and the center one transmitting and the center one and the right one receiving, and the center of the central coil aligned with the centerline of ROI.

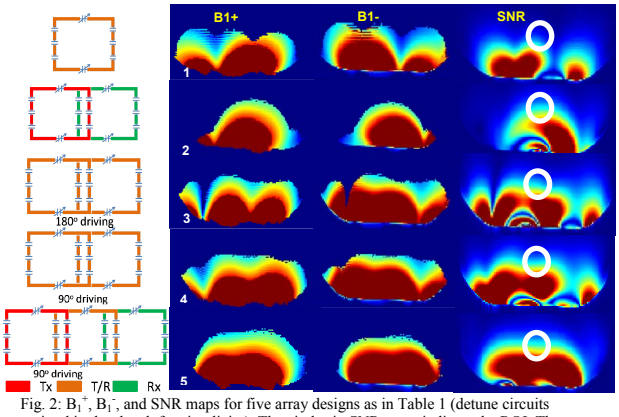

Fig. 2: B_1^+, B_1^-, and SNR maps for five array designs as in Table 1 (detune circuits omitted in the sketch for simplicity). The circles in SNR maps indicate the ROI. The windowing within each column is the same.

Experimental Validation: When loaded the tune and matching S_{11} of each coil was <-20dB and the isolation S_{21} between two neighboring coils were <-25dB. The unloaded/loaded Q ratio of a single element was 13.4. Resulting B_1^+, B_1^-, and SNR maps for the various designs are shown in Fig.2. From the B_1 maps, it is clear that for those designs utilizing TxRx offsetting (2 and 5), the peaks of B_1^+ coincide with the peaks of B_1^-, optimizing the system efficiency. Among all 5 arrays tested, the three element design achieved the highest average SNR within the ROI as well as the most homogeneous excitation within and near the ROI without any noticeable null regions in the FOV. This is also confirmed by the SNR profiles at two directions through the center of ROI as shown in Fig.3. Fig.3 also shows the necessity to optimize on 2D ROI rather than a line or a particular point given the fact that SNR of No.2 was close to No.5 at the vertical center line but performed much worse off-center along a horizontal profile. In comparing designs 3 and 4, we found that a 90° phase drive produced a higher B_1^+ efficiency in the ROI. This result is in contrast to those presented by Kraff *et al* [3] who claimed greatest B_1^+ efficiency near the coil overlap region with the coils drive with 180° phase difference. We find that 180° phase provides enhanced B_1^+ at shallow depths, but for deeper regions driving phases closer to 90° are superior, presumably due to more efficient excitation of a circularly polarized B_1^+ field. To illustrate the SAR benefit of quadrature excitation, temperature tests were performed on a 4kg leg of lamb with systems No.3 and No.4. The highest heating in each case was observed in the region of the coil overlap. With 90° phase drive (design No.4) there was 35% less peak local heating than with 180° phase (design No.3). This is understandable since the 180° phase drive results in currents *in* phase on the coil conductors on the overlapped edges, which will result in the E-fields associated with the capacitors there to be *in* phase also, yielding higher peak E-fields.

Conclusions

This abstract presents a prototype design of 7T spine coil design. By utilizing the concepts of TxRx offsetting, quadrature excitation, and quantitative optimization, this new design has improved B_1^+ efficiency and higher average SNR with the ROI, and less peak local heating compared with the other designs examined. Even with a two coil system as described by other authors [3] we find increased B1+ efficiency at depth and reduced SAR when the driving phase is optimized. The coverage along the length of the spine can be easily extended by adding more similar geometrically decoupled building blocks. The new techniques used in design optimization can also be generalized to other high field coil designs.

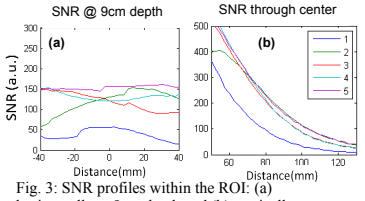

Fig. 3: SNR profiles within the ROI: (a) horizontally at 9cm depth and (b) vertically through the center

References

[1] Shapiro, MRI Clinics of North America 2006, 14(1):97-108. [2] Collins, et al, MRM 2002, 47:1026-28. [3] Kraff, et al, Invest. Radio.2009; 44(11): 734-740. [4] Wiggins, et al, ISMRM 2009, 2951. [5] Lattanzi, et al, ISMRM 2008: 1074. [6] http://www.fcc.gov/oet/rfsafety/dielectric.html. [7] Wang, et al, MRM 2002, 48:362-369. [8] Kumar, et al, MR Mater Phys. 2008 21:41-52